



**HAL**  
open science

# Supramolecular Assembly of Planar Systems from Modular Molecules with a Given Hydrophilic–Lipophilic Balance: Film Sensors with an Anthraquinone Signal Group

E. V. Ermakova, Alla Bessmertnykh-Lemeune, Michel Meyer, L. V. Ermakova, A. Yu. Tsivadze, V. V Arslanov

## ► To cite this version:

E. V. Ermakova, Alla Bessmertnykh-Lemeune, Michel Meyer, L. V. Ermakova, A. Yu. Tsivadze, et al.. Supramolecular Assembly of Planar Systems from Modular Molecules with a Given Hydrophilic–Lipophilic Balance: Film Sensors with an Anthraquinone Signal Group. *Protection of Metals and Physical Chemistry of Surfaces*, 2018, 54 (1), pp.6 - 18. 10.1134/S2070205118010057 . hal-01857121

**HAL Id: hal-01857121**

**<https://u-bourgogne.hal.science/hal-01857121>**

Submitted on 20 Dec 2021

**HAL** is a multi-disciplinary open access archive for the deposit and dissemination of scientific research documents, whether they are published or not. The documents may come from teaching and research institutions in France or abroad, or from public or private research centers.

L'archive ouverte pluridisciplinaire **HAL**, est destinée au dépôt et à la diffusion de documents scientifiques de niveau recherche, publiés ou non, émanant des établissements d'enseignement et de recherche français ou étrangers, des laboratoires publics ou privés.

# **Supramolecular Assembly of Planar Systems from Modular Molecules with a Given Hydrophilic–Lipophilic Balance: Film Sensors with an Anthraquinone Signal Group**

E. V. Ermakova,<sup>a</sup> A. G. Bessmertnykh-Lemeune,<sup>b</sup> M. Meyer,<sup>b</sup> L. V. Ermakova,<sup>a</sup>  
A. Y. Tsivadze,<sup>a</sup> and V. V. Arslanov<sup>a,\*</sup>

<sup>a</sup> Frumkin Institute of Physical Chemistry and Electrochemistry, Russian Academy of Sciences, Moscow, 119071 Russia

<sup>b</sup> Institut de Chimie Moléculaire de l'Université de Bourgogne (ICMUB), CNRS, Dijon, France

**Published on March 16, 2018 as an article in**

*Protection of Metals and Physical Chemistry of Surfaces* **2018**, *54*, 6–18

DOI: 10.1134/S2070205118010057

English translation of the original article published in Russian in  
*Fizikokhimiya Poverkhnosti i Zashchita Materialov* **2018**, *54*, 9–21

\* Corresponding author. E-mail: vladimir.arslanov@gmail.com

## **ABSTRACT**

This work presents an original approach to obtaining highly sensitive ultrathin film sensors that allows molecular design of surface-active modular molecules by completing a signal anthraquinone block with hydrophobic radicals and polar receptor groups, with their number and size provided in accordance with the sensor type. An important advantage of the suggested approach is that it not only allows the functioning of sensors in the aqueous medium, but also their manufacturing (supramolecular assembly). The key regularity of ligands of the suggested series is selectivity with respect to mercury and copper cations. Application of amphiphilic ligands in film liquid (Langmuir monolayers) and solid-state (Langmuir-Blodgett films) sensors allowed developing optical sensors for mercury and copper cations with the detection limit, as dependent on the sensor type, varying from several to hundredths of ppm.

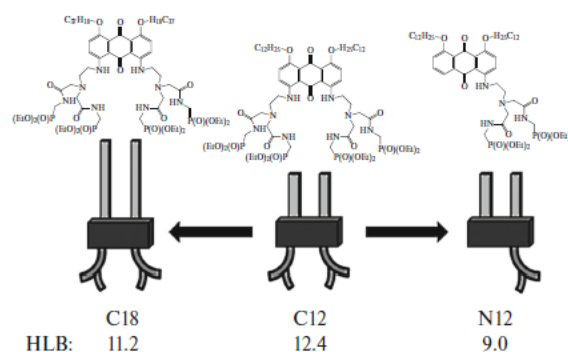
## 1. INTRODUCTION

In recent years, one of the most important problems of chemical science, which encompasses various spheres of human life, including health protection, is development of diagnostic systems [1–3]. These systems must provide the monitoring of harmful and dangerous ions and molecules both in the environment and in the human body. Among them, cations of such toxic metals as mercury, lead, cadmium, and copper that are powerful metabolic poisons for plants, animals, and human beings, are particularly dangerous. Herewith, mercury cations are considered as the most harmful inorganic substances [4, 5]. In the last hundred years, the amount of mercury in the upper 100 m of the World Ocean has doubled. The content of mercury in fish and in human hair in different countries of the world regularly exceeds the safe level [6]. Inorganic compounds of mercury are most widespread; they are extracted with solid particles or organic compounds. Hg(II) ions are bound both by organic and inorganic ligands and can be methylated. Such wide spreading of mercury in different objects in the ecosphere requires developing various detection methods, including high-sensitivity and high-precision ones. Therefore, development of efficient ligands for the binding of Hg<sup>2+</sup> simultaneously solving two problems: analytical (determination of Hg<sup>2+</sup> in aqueous media) and ecological (purification of aqueous solutions from this type of contamination [7–10]).

Copper is one of the important microelements that enter the human body. High copper concentrations stimulate generation of active oxygen forms, which results in oxidative damage to proteins and nucleic acids. However, this drawback of copper causes inactivation of the key antioxidant enzymes and results in disruption of energy processes in living systems [11, 12]. The content of copper in natural sources is relative low, but its concentration in water increases significantly due to corrosion of water-supply pipes. In this regard, the efforts of a significant part of the scientific community are aimed at development of systems of high-selectivity sensitive detection of mercury or copper cations, and other toxic metals in water that can irreparably damage the environment and human health.

This work presents a number of ligands (Scheme 1) containing the signal anthraquinone group, as well as hydrophilic and hydrophobic modules, and their number and size adjusted for development of stable and efficient thin film sensors for selective detection of mercury and copper cations in aqueous solutions. Molecular design was carried out according to two directions providing for an increase in lipophilicity of ligands for their application in ultrathin films: monolayers and Langmuir–Blodgett films. In the first case, the length of the hydrocarbon part of the molecule was lengthened by replacing two –OC<sub>12</sub>H<sub>25</sub> radicals (ligand C12) by –OC<sub>18</sub>H<sub>37</sub> (ligand C18); in the second case, the polar part of the molecule was decreased by

eliminating one hydrophilic receptor moiety while preserving the two hydrocarbon  $-\text{OC}_{12}\text{H}_{25}$  chains (ligand N12) (Scheme 1). One note that, when we developed this series of ligands, we attempted to preserve the architecture of classical amphiphilic molecules that provided a high level of molecular organization at interfaces.



**Scheme 1.** Chemical formulas of anthraquinone ligands with different lipophilicity, the corresponding schematic images and HLB values calculated according to the Griffin method [13].

## 2. EXPERIMENTAL

Synthesis of ligands was carried out according to the methods described in [14]; the physico-chemical characteristics of the obtained compounds correspond to those published earlier [15]. Chloroform (analytical grade) (Merck) was distilled over  $\text{CaH}_2$ . Hexahydrates of copper(II) and mercury(II) perchlorates (98%, Aldrich) were used without any additional purification. Ligand solutions (0.1 mM) were prepared by sample dissolution in chloroform.

The subphase used was deionized water (18  $\text{M}\Omega$  cm, Vodolei, NPP Khimelektronika) or aqueous solutions of perchlorates. Gilson Distriman microsamplers were used for application of monolayer-forming solutions. Compression isotherms of monolayers were obtained using 1000-2 KSV Minitrough setup (Finland) equipped by a Teflon Langmuir trough, polyacetal hydrophilic barriers, a Wilhelmy plate (platinum plate) for determination of the surface pressure of the monolayer, and a device for automated transfer of monolayers to solid substrates. Transfer of monolayers to solid substrates was carried out using the Langmuir–Blodgett method with constant surface pressure.

Electronic-absorption spectra of monolayers on the aqueous subphase surface in the wavelength range of 200–800 nm were registered using a fiber-optic AvaSpec-2048 FT-SPU spectrophotometer (Netherlands). A reflectometric UV/VIS tester with the fiber diameter of

400  $\mu\text{m}$  joined together with a six-fiber irradiating cable was positioned normally to the studied surface at the distance of 3 mm from the monolayer.

Electronic-absorption spectra of films supported on the surface of quartz substrate were recorded using a SHIMADZU-2450 spectrometer (Japan) in the wavelength range of 200–900 nm.

### 3. RESULTS AND DISCUSSION

#### 3.1. Monolayers of Amphiphilic C12, C18, and N12 Ligands on the Surface of Deionized Water

Using amphiphilic ligands in sensors with sensitive elements in the form of ultrathin films on the liquid (water) surface has a triple goal: (1) determination of complexing properties of ligands in labile organized systems with the uniform orientation of functional groups (2D transition systems between the solution and solid substrate), (2) preorganization and assembly of chromoionophores in monolayers at the air/water interface for their further transfer to solid substrates using the Langmuir–Blodgett method, and (3) development of liquid sensors for the purposes of nano(micro)fluidics. Obviously, these directions imply analysis of the processes of cation binding by ligand monolayers from the subphase.

Figure 1a shows compression isotherms of monolayers of three ligands C12, C18, and N12 on the surface of water (pH 5.5). The analysis of compression isotherms of these polyfunctional molecules is expedient to carry out taking into account the influence of each of the three modules: (1) Hydrophobic (hydrocarbon chains), (2) Signal (planar anthraquinone fragment, more hydrophobic than hydrophilic), and (3). Polar (one or two hydrophilic chains of branched [(acetylamino)methyl]diethoxyphosphoryl groups).

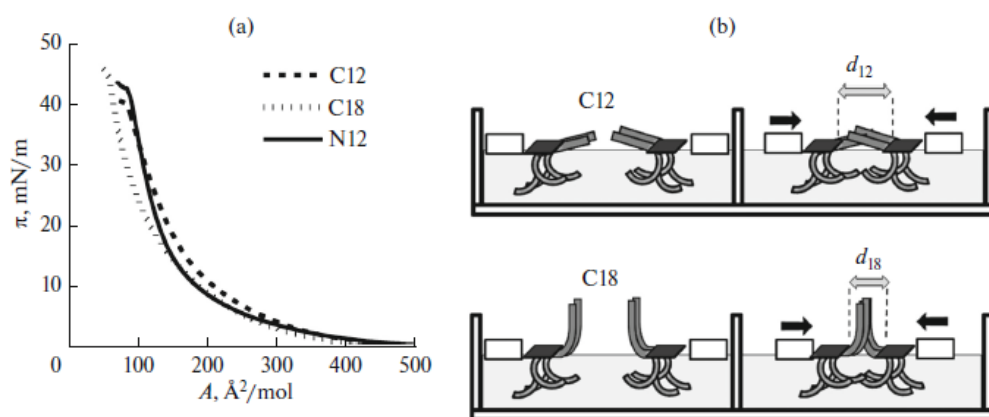


**Fig. 1.** (a) Compression isotherms of monolayers of three ligands C12, C18, and N12 deposited on a water surface. (b) Scheme explaining lower surface areas occupied by the monolayer of

the C18 ligand as compared to the monolayer of the C12 ligand.  $d_{12}$  and  $d_{18}$  are distances between anthraquinone groups of the corresponding ligands in the monolayer at the given surface pressure value ( $d_{12} > d_{18}$ ).

The proximity of isotherms and high values of the limiting surface area of all three related compounds indicates a certain conservatism in the development of molecules with rather different structures. The observed high limiting areas per single molecule for condensed states of the monolayer indicate that the anthraquinone fragment is located in parallel to the subphase surface (according to the model, its area is  $100 \text{ \AA}^2$  [16]) and that at high surface pressures bulk polar groups can occupy areas commensurable with the aromatic fragment. Obviously, the polarity (hydrophilicity) values of ether oxygens and oxygen of the carbonyl group are enough to “lay down” the anthraquinone fragment onto the surface into the “face-on” position already in the course of monolayer formation. Usually, when monolayers are compressed, flat aromatic fragments are displaced from the interface surface and their planes in the condensed state are arranged normally to the subphase surface, i.e., they assume an “edge-on” orientation owing to the energy gain owing to the  $\pi$ - $\pi$  stacking interactions. Here, low values of the monolayer area are registered. They correspond to this very orientation of aromatic moieties of the molecules [17–21].

Nevertheless, the observed slight difference in the shape and position of compression isotherms allows correlating molecular construction of the ligand and its organization in the monolayer on the surface. Firstly, one must point out that transition from C12 to C18 leads to a shift of the isotherm towards lower areas and an increase of the collapse pressure; here, the shape of isotherms is preserved. Secondly, transition from ligand C12 to N12, for which a single branched polar group remains instead of two, results in a steeper rise of the curve at lower surface areas in the condensed state.

Taking into consideration that both the signal group and polar groups of the C12 and C18 ligands immersed into the subphase manifest close organization on the water surface, the above shift in the isotherm of C18 into the condensed region can be due only to an increase in the length of the hydrocarbon radical turned toward the air phase. Therefore, despite the complexity of parts of modular molecules attached to the “tails,” the difference in the length of the latter produces a similar effect on the behavior of monolayers, as in the case of fatty acids with the corresponding chain size (e.g., lauric and stearic acids). However, as seen in Fig. 1a, in the presence of polar modules with an area significantly exceeding the area of the cross section of the hydrocarbon radical, the effect of the difference in the chain length is much lesser than in

the case of fatty acid monolayers. The C18 isotherm is only slightly shifted toward lower areas as compared to the C12 isotherm, which is explained by an increase in the contribution of interchain interactions at an increase in the “tail” length. The scheme (Fig. 1b) shows fragments of C12 and C18 monolayers explaining the higher degree of monolayer condensation of the ligand with a long chain. Obviously, in this case, the bulky polar groups prevent full implementation of the contribution of interchain interactions (as in the case of fatty acid monolayers), not allowing hydrocarbon chains to approach each other to the required distance even at high monolayer compression degrees.

Thus, the ligands of the suggested series, owing to the architecture of classical amphiphilic molecules, form stable monolayers at the air/water interface. Here, comparison of the shape and position of compression isotherms of the three ligands point to the fact that rigidity of their monolayers is determined by the anthraquinone fragment preserving the horizontal position on the surface of water in the course of the whole compression process; an increase in the length of the hydrocarbon radical in the molecule enhances condensation of the monolayer, just as does elimination of one polar group from the molecule, which provides a closer contact between the planar signal groups in the “face-on” orientation.

### *3.2. Monolayers of Amphiphilic Ligands C12, C18, and N12 on the Surface of Aqueous Solutions Containing Mercury and Copper Cations*

Langmuir monolayers offer a unique possibility to study complexation in an aqueous medium of ligands that are insoluble in water (or form very dilute solutions). In the case of the sensors considered in this work, this allows determining the performance and selectivity of the binding of inorganic analytes. Such interactions play the key role in obtaining hybrid metal–complex monolayers for the further formation of Surface-Anchored metal-organic frameworks (SURMOFs) [22, 23].

Figure 2a demonstrates the effect of mercury cations in the subphase (1 mM) on the compression isotherms of the C12, C18, and N12 monolayers. Interaction with mercury cations causes a shift in all isotherms toward lower areas. Obviously, these interactions limit the freedom of movement of polar groups, which imparts higher compactness to the thus-formed sublayer.

Thus, addition of mercury cations causes condensation of monolayers same as in the case of fatty acids [24]. However, shrinkage of fatty acid monolayers originated from a compensation of negative charges of carboxylate headgroups in the presence of positively charged metal ions. On the other hand, the authors observed strong expansion of monolayers due to electrostatic

repulsion of positively charged complexes in the studies of the binding of transition metal cations by monolayers of dicycliclone [25, 26] or *tert*-butylthiacalixarene [27, 28]. The studied ligands do not bear any negative charges, as opposed to acids, and, in the case of the binding of cations, the behavior of their monolayers should bring to mind the behavior of dicycliclone monolayers, i.e., expansion of the monolayer. The observed shrinkage indicates a different mechanism. Obviously, the bulkiness of polar nodes decreases considerably in the case of the binding of the cations and mobility of “brushes” is limited. Here, this effect must be enhanced at an increase in the cation concentration in the subphase. Figure 2b shows as an example compression isotherms for the C12 ligand monolayer on the surface of the aqueous subphase containing different concentrations of  $\text{Hg}(\text{ClO}_4)_2$ . One can see that isotherms are consistently shifted toward smaller areas and the compression modulus increases at an increase in the concentration of  $\text{Hg}^{2+}$  cations in the subphase. Such a behavior of monolayers in the course of the binding of cations is also characteristic for the two other ligands.

The scheme presented in Fig. 2c explains the effect of the concentration of mercury cations in the subphase on the change in the monolayer structure and, accordingly, on the position and shape of compression isotherms. Before interaction with the cations, polar groups of “brushes” are in chaotic motion, occupy a large volume, and prevent the drawing together of lipophilic groups on the surface near the air phase. The binding of cations deprives the “brushes” of mobility and results in monolayer shrinkage. At an increase in the concentration of mercury cations in the subphase, an ever-higher number of modes is involved in this process and the monolayer shrinkage is greater. An important difference between the receptors located directly on the water surface (dicycliclone, *tert*-butylthiacalixarene) and immersed into the aqueous subphase (the ligands considered here) consists in a more effective compensation of the complex charge by counterions in the latter case. This effect also contributes to the monolayer shrinkage.

Thus, compression isotherms of monolayers of all ligands change regularly when mercury cations are introduced into the subphase. However, as we showed in [19, 20], the change in the compression isotherms of monolayers after addition of metal cations into the subphase provides no unambiguous answer as to the presence of complexation in the system. The shift in the  $\pi$ - $A$ -curves as a result of addition of cations may be related to film reorganization due to physical adsorption of charged particles, changed of double electric layer characteristics, etc. Besides, it is possible that the isotherms do not change their position as a result of compensation of effects caused by complexation. At the same time, spectral shifts for the systems with complexation

are always pronounced. In this connection, information on complexation was obtained using in situ fiber-optic reflectance-absorption spectroscopy of monolayers.

Figure 3a demonstrates the effect of the compression degree (a surface density) of the monolayer on a pure water surface on the intensity and position of the electronic spectrum of the ligand. One can see that, when the density of the C12 ligand monolayer increases in the course of its compression, only the intensity of the absorption band increases and the position of  $\lambda_{\max} = 560$  nm remains unchanged. Let us note that  $\lambda_{\max}$  coincides with the position of this band in the spectrum of the C12 solution in water. First, this indicates the absence of aggregation of C12 in the monolayer even at high surface concentrations and, secondly, to the correctness of the suggested organization of ligand monolayers (Figs. 1b, 2c), according to which signal groups of ligand molecules in both systems are in close contact with the aqueous phase. The same is indicated by the large value of the monolayer area in the condensed region, which is almost three times higher than the calculated area for the edge-on anthraquinone fragment (or two hydrocarbon chains) and is by 30–40% greater than the face-on positioned anthraquinone part of the molecule.

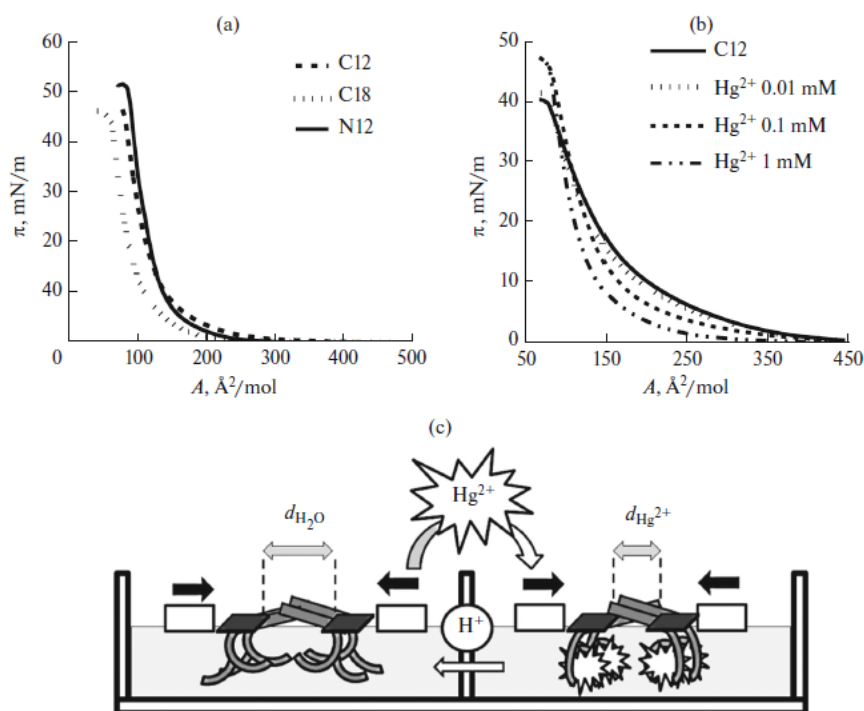


**Fig. 2.** (a) Compression isotherms of monolayers of three ligands, C12, C18, and N12, deposited on a 1 mM  $\text{Hg}(\text{ClO}_4)_2$  aqueous solution. (b) Compression isotherms of monolayers of the C12 ligand deposited on a  $\text{Hg}(\text{ClO}_4)_2$  aqueous solution of different concentration. (c)

Scheme demonstrating the change in the structure of a monolayer of the C12 ligand upon binding of the  $\text{Hg}^{2+}$  cations (2 eqs.) and explaining its shrinkage ( $d_{\text{H}_2\text{O}} > d_{\text{Hg}^{2+}}$ ).

The presented data are obtained under the conditions when interaction of the  $\text{Hg}^{2+}$  cations with the ligand monolayer occurs in the subphase already containing these cations (Fig. 3b). The binding of mercury cations by the C12 ligand is registered directly after the solution spreads over the surface and the solvent evaporates (15 min): the absorption maximum of the monolayer on the pure water surface ( $\lambda_{\text{max}} = 560 \text{ nm}$ ) shifts hypsochromically by 25 nm and the band intensity increases in the course of the monolayer compression, while its position is preserved. Therefore, no aggregation occurs in the monolayer even at high surface concentrations even when complexes are formed.

We changed the experiment so as to determine the kinetics of the binding of mercury cations by the C12 monolayer. First, a monolayer was formed on the pure water subphase; then, it was compressed to  $\pi = 12.5 \text{ mN/m}$ ; and, after this, mercury cations were added by replacement of the subphase and their concentration was adjusted to 1 mM. As seen in Fig. 4a, monolayer compression on the pure water surface from  $\pi = 0$  to  $\pi = 12.5 \text{ mN/m}$ , just as in the previous experiments, results in growth of the absorption intensity without any shift in the bands. After the cations are added into the subphase, the characteristic band corresponding to the pure ligand instantaneously shifts hypsochromically by  $\sim 25 \text{ nm}$ , which indicates formation of the complex. When this monolayer is compressed, absorption intensity increases and a slight bathochromic band shift related to establishment of the equilibrium in the system is observed.

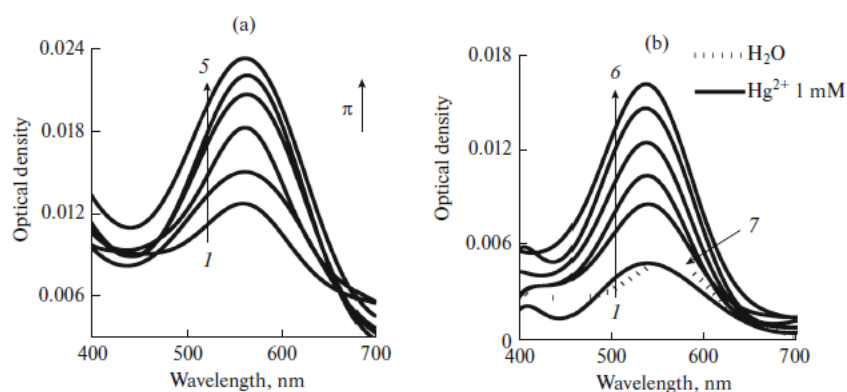


**Fig. 3.** Effect of the surface pressure on the *in situ* electronic-absorption spectra of the C12 ligand monolayer deposited on (a) a water surface and (b) on a 1 mM  $\text{Hg}(\text{ClO}_4)_2$  aqueous solution. Surface pressure of monolayer (a): (1) 5, (2) 10, (3) 20, (4) 25, (5) 30 mN/m. Surface

pressure of monolayer (b): (1, 7) 5, (2) 15, (3) 20, (4) 25, (5) 30, (6) 35 mN/m, (7) the ligand monolayer deposited on a deionized water.

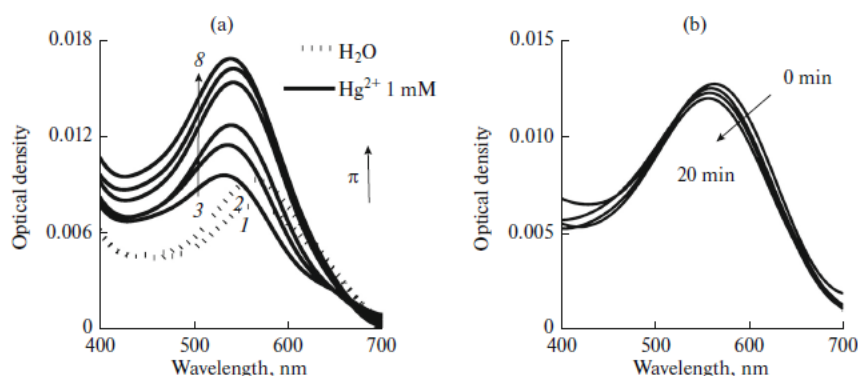


**Fig. 4.** *In situ* electronic-absorption spectra of the C12 ligand monolayer (a) (1, 2) deposited on a water surface, (3–8) after addition of the Hg(ClO<sub>4</sub>)<sub>2</sub> salt (1 mM) into the subphase. Surface pressure of monolayer (a): (1) 5, (2) 12.5, (3) 12.5, (4) 15, (5) 20, (6) 35, (7) 50, (8) 42 mN/m. (b) Shift of the electronic-absorption spectra of the C12 ligand monolayer at an increase in the monolayer conditioning time on the surface of 0.01 mM Hg(ClO<sub>4</sub>)<sub>2</sub> solution from 5 to 20 min, π = 10 mN/m.

The change in the surface pressure in the range of 10–15 mN/m at the mercury cation concentration in the subphase of 0.1 mM (the second method) produces practically no effect on the rate of the complexation reaction. At another tenfold decrease in the concentration (0.01 mM), the binding rate for π = 10 mN/m decreases by almost six times (Fig. 4b).

Therefore, complexation in the C12 monolayer for mercury ion concentrations  $C > 0.1$  mM occurs at high rates, which indicates high availability of functional groups (receptor modules) in sensors of this type. Let us also point out that the binding of cations in the sublayer of polar groups resulting in an increase in polarity of this part of the monolayer causes no reconstruction of the monolayer structure. In [20], in the studies of the monolayer of the macrocyclic pentaaminoanthraquinone we observed a change in the orientation of an anthraquinone fragment from the planar one (face-on) to the vertical one (edge-on) that is caused by immersion of the macrocyclic receptor fragment into the aqueous subphase as a result of protonation of its amino groups. Obviously, this effect is not implemented in this case and the anthraquinone group preserves its orientation on the surface, which prevents aggregation of the aromatic module.

When compression isotherms of the C12 and C18 monolayer on the surface of pure water (Fig. 1a) were compared, it was shown that the ligand with a longer chain provides a more condensed monolayer:  $A_{\text{lim}} = 140 \text{ \AA}^2$  for C18 and  $A_{\text{lim}} = 200 \text{ \AA}^2$  for C12. Therefore, despite the fact that the large size and branched structure of polar groups similar for both ligands and also the horizontal orientation of the anthraquinone group are responsible for the large monolayer areas, the hydrocarbon radical affects the monolayer organization: the longer hydrocarbon “tail” of C18 enhances the monolayer condensation. The same tendency is also preserved for monolayers on the surface of the aqueous mercury salt solution and the differences in the limiting areas of monolayers of the two ligands decrease:  $110 \text{ \AA}^2$  for C18 and  $140 \text{ \AA}^2$  for C12 at  $[\text{Hg}^{2+}] = 1 \text{ mM}$ .

Spectroscopic studies of the binding of mercury cations by monolayers of the C18 ligand showed that, just as for the C12 monolayer, interaction between mercury cations and the monolayer of its long-chain counterpart causes a hypsochromic shift of the main ligand band at  $\Delta\lambda = 25 \text{ nm}$  (Fig. 5). Thus, monolayers of the C12 and C18 ligands differing only in the length of the hydrocarbon radical bind mercury cations from the subphase with similar efficiency.

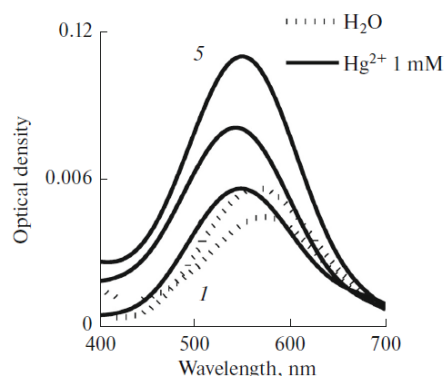


**Fig. 5.** *In situ* electronic-absorption spectra of a monolayer of the C18 ligand (1, 2) deposited on a water surface and (3–5) on the surface of the aqueous 1 mM solution of the  $\text{Hg}(\text{ClO}_4)_2$  salt. Surface pressure of the monolayer: (1) 5, (2) 12.5, (3) 12.5, (4) 20, (5) 30 mN/m.

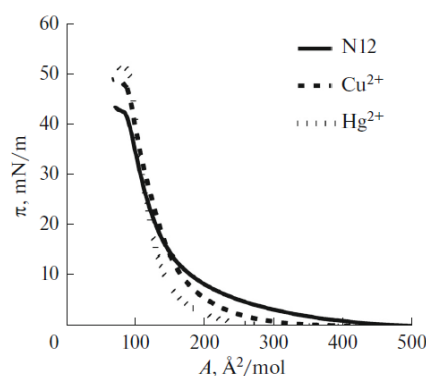


**Fig. 6.** Compression isotherms of N12 monolayers deposited on a pure water surface (N12) and on a 1 mM aqueous solution of  $\text{Cu}(\text{ClO}_4)_2$  and  $\text{Hg}(\text{ClO}_4)_2$ .

In the case of monolayers of the N12 ligand, addition of mercury and copper cations into the subphase results in a shift of isotherms into the region of small areas for  $\pi < 15 \text{ mN/m}$ . In the

range of high surface pressures, the isotherms do not differ much and the isotherms for cation-containing subphases manifest higher destruction pressures and rigidity (Fig. 6).

Nevertheless, one should emphasize that, in the case of mercury cations, the shrinkage, rigidity, and monolayer-destruction pressure are higher than in the case of copper cations. These data indicate that a more compact monolayer is formed in the first case and that, if these changes are due to complexation, then its mechanisms differ for the two systems. At least, one must state that, in accordance with the coordination numbers of these cations, a larger number of functional groups participates in formation of the coordination sphere of  $\text{Hg}^{2+}$  than in the case of  $\text{Cu}^{2+}$ .

Complexation was studied using electronic absorption spectra of N12 monolayers on the corresponding subphases. Figure 7a shows the effect of copper cations in the subphase on the electronic-absorption spectra of the N12 monolayer in the case of the second method of addition of cations. One can see that addition of copper cations under the formed monolayer leads to the bathochromic band shift by 52 nm. The absorption spectra of the monolayer on the surface of the aqueous subphase containing mercury cations is shifted in the opposite direction, i.e., hypsochromically, by 34 nm (Fig. 7b). First of all, one must note that the value of the hypsochromic shift of the main band for the N12 monolayer as a result of complexation ( $\Delta\lambda_{\text{max}}$ ) with mercury cations corresponds to the value of this shift for the C12 and C18 ligands. This reflects the similarity both in the complexation mechanism and in the structure of the forming complexes for the three ligands. In the case of the binding of copper cations by the N12 monolayer,  $\lambda_{\text{max}}$  is shifted bathochromically and to a much greater value than in the case of  $\text{Hg}^{2+}$ , which indicates implementation of a different type of interactions with participation of other functional receptor groups. We suggest that the binding of copper and mercury cations by the molecules of N12 and C12 (C18) occurs in accordance with the reactions shown in Scheme 2.

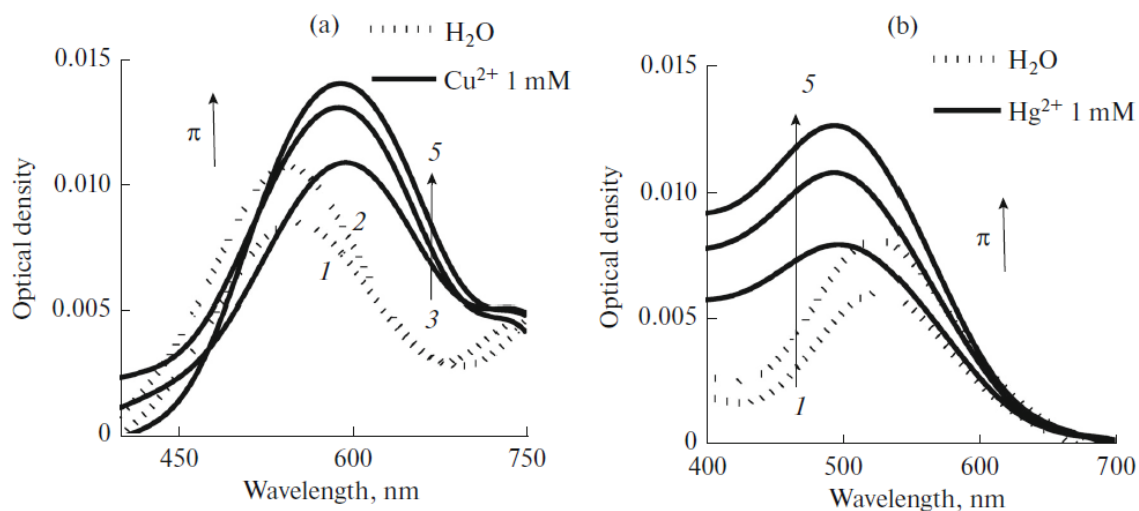
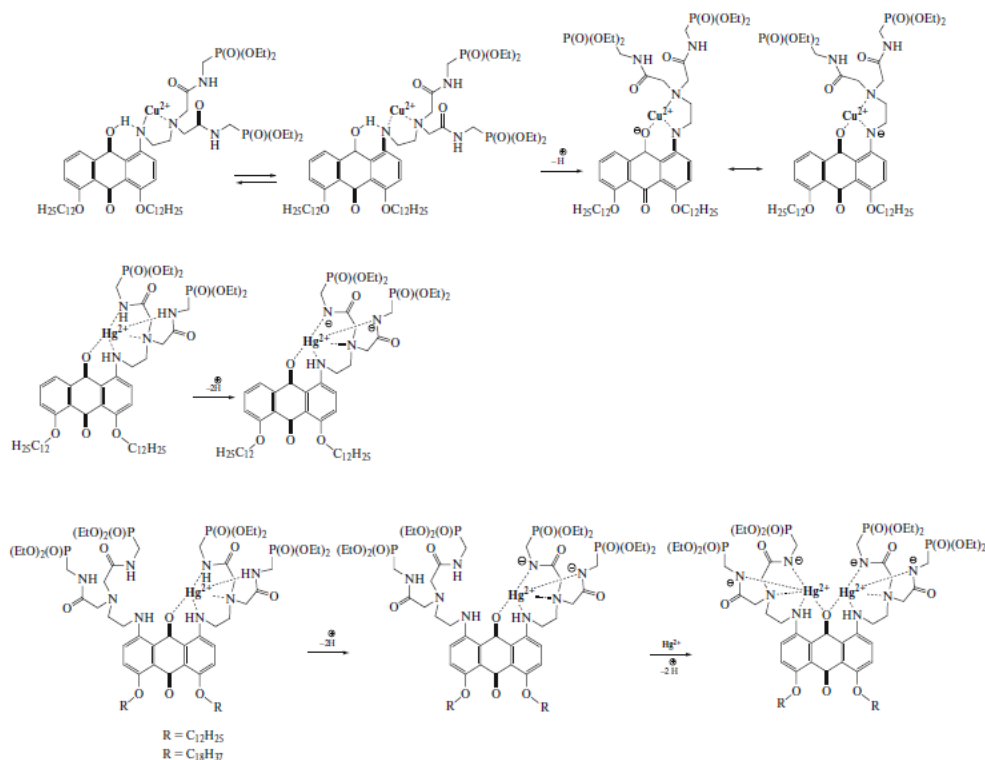


**Fig. 7.** *In situ* electronic-absorption spectra of a monolayer of the N12 ligand (*I*, *2*) deposited on a water surface and on the surface of the water subphase containing (a) 1 mM Cu(ClO<sub>4</sub>)<sub>2</sub> solution or (b) 1 mM Hg(ClO<sub>4</sub>)<sub>2</sub> solution. Surface pressure of monolayer (a): (*I*) 5, (*2*) 10, (*3*) 10, (*4*) 25, (*5*) 40 mN/m. Surface pressure of monolayer (b): (*I*) 5, (*2*) 10, (*3*) 10, (*4*) 15, (*5*) 30 mN/m.



**Scheme 2.** Binding of copper and mercury cations by the N12 and C12 (C18) molecules and the structure of the forming complexes.

Unfortunately, it appears impossible to confirm the structure of the complexes, as no crystals of these compounds can be grown. Nevertheless, one can state that the binding of copper cations is accompanied by deprotonation of aromatic amino groups conjugated with the signal fragment and amide groups of the polar ligand nodes undergo deprotonation in the course of coordination in the case of mercury cations.

### 3.3. Selectivity and Regeneration of Sensor Monolayers from the C12, C18 and N12 Chromoionophores

We showed earlier that the compression isotherms of the three ligands, though they yield information on organization of molecules in the film, but change negligibly and consistently when the cations are bound. This does not allow using the characteristics of compression isotherms for determination of selectivity of the liquid sensor with respect to metal cations.

The selectivity of sensors was determined using the method of fiber optic spectroscopy by successive addition to the subphase of the  $\text{Cu}^{2+}$ ,  $\text{Pb}^{2+}$ ,  $\text{Cd}^{2+}$ ,  $\text{Ca}^{2+}$ , and  $\text{Hg}^{2+}$  cations. As is seen in fig. 8, the presence of cations of metals from different groups of the periodic system (with the exception of  $\text{Hg}^{2+}$ ) in a C12-ligandbased sensor produces practically no shift in the electronic-absorption spectra of monolayer absorption. A slight hypsochromic shift (3 nm) caused a change in the ionic composition of the monolayer due to physical adsorption of cations. When  $\text{Hg}^{2+}$  cations are added to the mixture, the spectrum shifts hypsochromically by 20 nm.

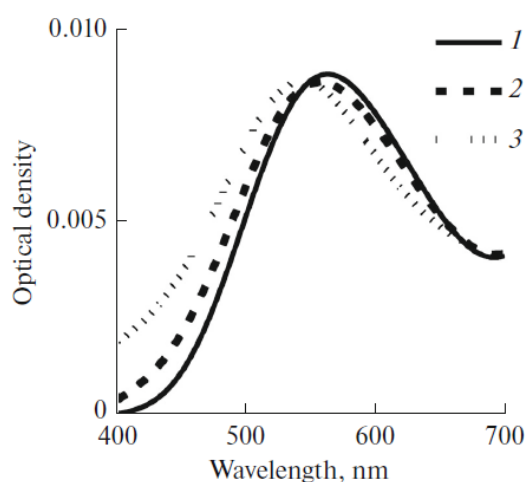


**Fig. 8.** *In situ* electronic-absorption spectra of a monolayer of the C12 ligand (1) deposited on the surface of pure water before and after sequential addition of transition metal cations,  $[\text{M}^{2+}] = 1 \text{ mM}$ : (2)  $\text{Cu}^{2+} + \text{Pb}^{2+} + \text{Cd}^{2+} + \text{Ca}^{2+}$ ; (3)  $\text{Cu}^{2+} + \text{Pb}^{2+} + \text{Cd}^{2+} + \text{Ca}^{2+} + \text{Hg}^{2+}$  at the constant surface pressure value of 10 mN/m.

Selectivity of the binding of  $\text{Hg}^{2+}$  cations by the monolayer of the long-chain C18 ligand was determined in the same way as for the C12 monolayer, by successive addition into the subphase of the  $\text{Cu}^{2+}$ ,  $\text{Pb}^{2+}$ ,  $\text{Ca}^{2+}$ ,  $\text{Cd}^{2+}$ , and  $\text{Hg}^{2+}$  cations. These studies led to a similar result: the binding of mercury cations occurs with the same high performance.

Interesting results were obtained by studying a competitive binding of  $\text{Hg}^{2+}$  and  $\text{Cu}^{2+}$  cations by the N12 monolayer (Fig. 9). No band shift was observed after monolayer compression to 10 mN/m and addition of lead, calcium, and cadmium cations (Fig. 9a, 2). Introduction of copper (Fig. 9a, 3) and mercury (Fig. 9b, 4) causes a shift in the spectrum of the pure ligand monolayer, accordingly, into the red and blue ranges. Moreover, in the case when  $\text{Hg}^{2+}$  cations are added after  $\text{Cu}^{2+}$  cations, the spectrum shifted into the red region as a result of complexation of the ligand with Cu(II) undergoes a hypsochromic shift. In the case of the reverse sequence of addition of these cations, the spectrum that has shifted hypsochromically after addition of  $\text{Hg}^{2+}$ , does not change its position after addition of Cu cations. Therefore,  $\text{Hg}^{2+}$  cations can substitute  $\text{Cu}^{2+}$  cations in the complex, but not vice versa. This result indicates that the complex of the ligand with mercury cations possesses a higher binding constant than does the ligand– $\text{Cu}^{2+}$  complex.

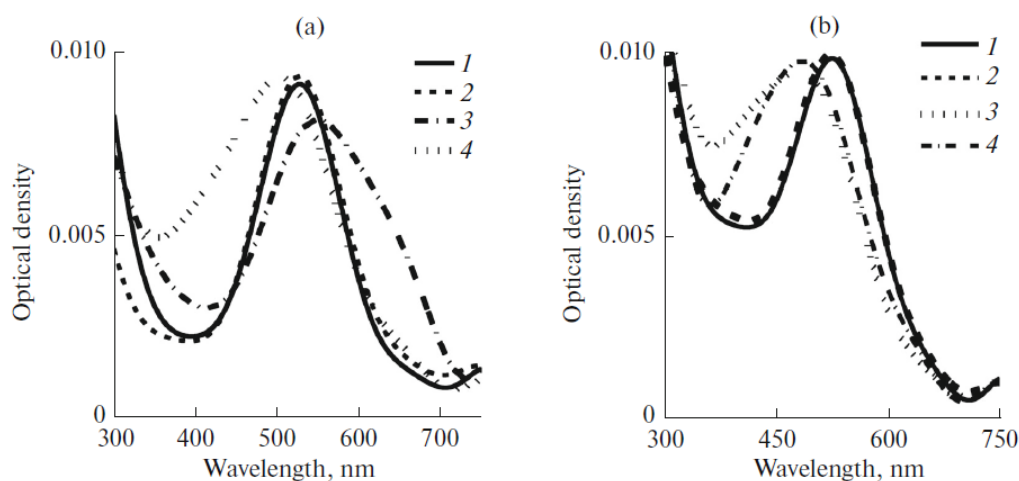


**Fig. 9.** *In situ* electronic-absorption spectra of a monolayer of the N12 ligand (1) deposited on the surface of pure water before and after sequential addition of transition metal cations,  $[\text{M}^{2+}] = 1 \text{ mM}$ : (a) (2)  $\text{Pb}^{2+} + \text{Cd}^{2+} + \text{Ca}^{2+}$ , (3)  $\text{Pb}^{2+} + \text{Cd}^{2+} + \text{Ca}^{2+} + \text{Cu}^{2+}$ , (4)  $\text{Pb}^{2+} + \text{Cd}^{2+} + \text{Ca}^{2+} + \text{Cu}^{2+} + \text{Hg}^{2+}$ ; (b) (2)  $\text{Pb}^{2+} + \text{Cd}^{2+} + \text{Ca}^{2+}$ , (3)  $\text{Pb}^{2+} + \text{Cd}^{2+} + \text{Ca}^{2+} + \text{Hg}^{2+}$ , (4)  $\text{Pb}^{2+} + \text{Cd}^{2+} + \text{Ca}^{2+} + \text{Hg}^{2+} + \text{Cu}^{2+}$  at the constant surface pressure value of 10 mN/m.

Regeneration of monolayers of the N12–M<sup>2+</sup> complexes was carried out by acidification of the subphase (HCl, 0.1 M, pH 2), which resulted in dissociation of the complex and a shift in the absorption band to the position corresponding to the ligand band. The further neutralization of the subphase to pH 5.5 (NaOH, 0.1 M) brought back the ability of monolayers to bind mercury cations (Fig. 10).

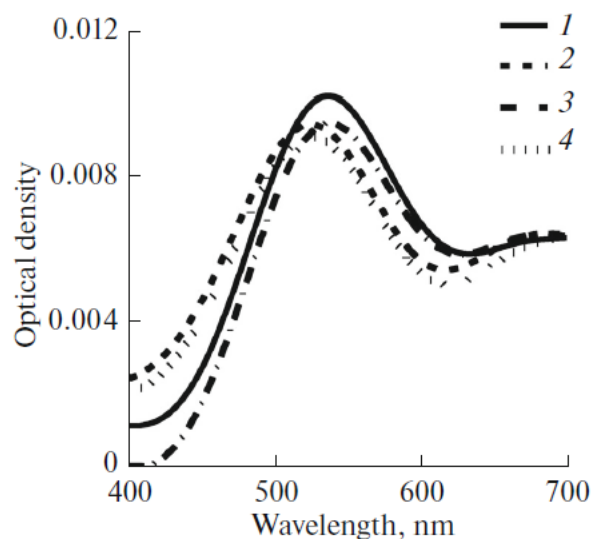


**Fig. 10.** Regeneration of the N12–Hg complex in the monolayer deposited on a water surface: (1) N12 monolayer on the surface of water, (2) in the presence of mercury cations (1 mM) in the subphase, (3) dissociation of the complex after acidification with HCl (0.1 M, pH 2), (4) neutralization of the subphase by NaOH (0.1 M, pH 5.5) resulting in reduction of the complex.

We showed above in analysis of compression isotherms that the behavior of monolayers at high compression degrees is determined by anthraquinone fragments in the “face-on” orientation and that implementation of such a structure requires compression of branched polar nodes (“brushes”). Obviously, under these conditions, steric limitations can appear that hinder formation of the coordination sphere characteristic for ligand and cation complexes both in the solution and in the monolayer at low surface pressure values. The effect of this factor was studied using electronic-absorption spectra of monolayers. After monolayer compression to  $\pi = 10, 15, \text{ and } 20 \text{ mN/m}$ , cations were introduced into the subphase. It was found that they were binding in the case of the cation concentration not exceeding 1 mM occurred practically instantaneously at all surface pressure values. Kinetic studies showed that the complexation time increases significantly at a decrease in the cation concentration; here, the surface pressure produces practically no effect on the reaction rate.

The importance of results obtained in this section consists not only in the fact that they represent the first detailed studies of complexation in monolayers for the hierarchical series of chromoionophores and different cations. The suggested study protocol allows one to obtain reliable information as to implementation of the complexation process in Langmuir monolayers, which demonstrates the correctness of the above consideration on the necessity of supplementing thermodynamic data (compression isotherm) with data of fiber-optic spectroscopy. Although we have earlier pointed out this rather obvious conclusion [19, 20], in this work, owing to spectral regularities of the behavior of the N12 ligand monolayers in the case of the binding of mercury and copper cation, the obtained result appears not only useful, but also rather elegant.

#### *3.4. Langmuir–Blodgett Films (LB films) of Chromoionophores C12, C18, and N12*

The Langmuir–Blodgett method is one of the most perfect tools capable of collecting functional multilayer structure of monolayers with a given molecular organization and composition on solid substrates. It is used to solve many modern problems of nanotechnology and supramolecular chemistry, such as substrate-induced patterning [29, 30], lateral LB films patterning using the approaches of soft-gel lithography [31], immobilization of active molecules in mesh matrices [32], development of miniature chemical sensors [33–35], and development of optical and electronic nanodevices [36–38].

Certain originality is possessed by recent works on the development of sensors (test strips) based on LB films for visual determination of Cd<sup>2+</sup> cations [39, 40]. Owing to high extinction of the ligands, already a 16-dye monolayer with the protective polymer layer provides sufficient sensitivity for determination of cadmium cation with the unaided eye. Nevertheless, the problem of obtaining high-quality LB films from nodular molecules remains rather acute. The ease of formation of multilayer highly ordered LB films from classical amphiphilic molecules does not also guarantee obtaining a similar structure for amphiphilic molecules of complex structure. This in full measure also concerns the ligands studied in this work.

Variation in wide limits of various parameters responsible for obtaining films of the C12 ligand did not lead to development of stable organized multilayer systems (Table 1). The main fault of the obtained LB films is their partial washing away when they are conditioned in water or aqueous solutions of metal salts.

One must note that, despite the higher stability of monolayers on the water surface, the above regularities of their organization determined by the ligand structure did not allow obtaining multilayer films on solid substrates with the required level of organization. Monolayer transfer

coefficient ( $\varphi$ ) varied in wide limits and in the case of the substrates movement above the  $\varphi$  value were higher than in the case of its immersion into the subphase. The LB films quality could be improved when not pure-ligand monolayers were transferred, but those of its complex with mercury cations, which caused enhancement of the compactness and a decrease in the mobility of polar nodes. Ultimately, the transfer coefficient of monolayers of the complex increased by at least 50%. The further operation regarding dissociation of complexes carried out by the conditioning of LB films in an acidic solution (HCl) provided recovery of the ligand efficiency. However, this procedure resulted in the washing away of a considerable amount of film from the substrate surface.

Transition from C12 to more lipophilic ligands C18 allowed significantly enhancing the stability of LB films with respect to washing. The method of spectrophotometry allowed establishing that, in the case of the C12 ligand, up to 50% of LB films is washed away from the quartz surface after 20 s of conditioning in water, while only 20% and 24% of C18 and N12 LB films is washed away in this time.

**Table 1.** Parameters of ligand monolayers transfer onto solid substrates using the Langmuir–Blodgett technique

	Parameters	Conditions
1	Ligand	C12
2	Nature of the substrate	Quartz plate (20 × 10 mm), silicon substrate (20 × 10 mm), cover glass (20 × 20 mm)
3	Number of layers	2, 5, 7, 10, 18
4	Transfer surface pressure	10, 15, 20, 30 (mN/m)
5	Dipping speed of the substrate: up/down	1, 5, 10 mm/min
6	Rate of monolayer compression	5, 8, 9, 10, 15 mm/min
7	Transfer ratio	Up: –0.5 to 1.5 Down: –0.7 to 0

Enhanced stability of multilayer LB films of C18 produces a positive effect also on the operation of the solid-state film sensor based on this ligand. As seen in Fig. 11, the rate of the washing away of the film formed by the C18 ligand is much lower than that in the case of a short-chain counterpart. The detection limit of copper cations by LB films based on the C12 and C18 ligands is  $10^{-7}$  M, which is for 100 times higher than the detection limit of mercury cations by monolayers of ligands on the air/water interface ( $10^{-5}$  M). Therefore, using ligands with elevated lipophilicity allowed enhancing stability and sensitivity of LB films.

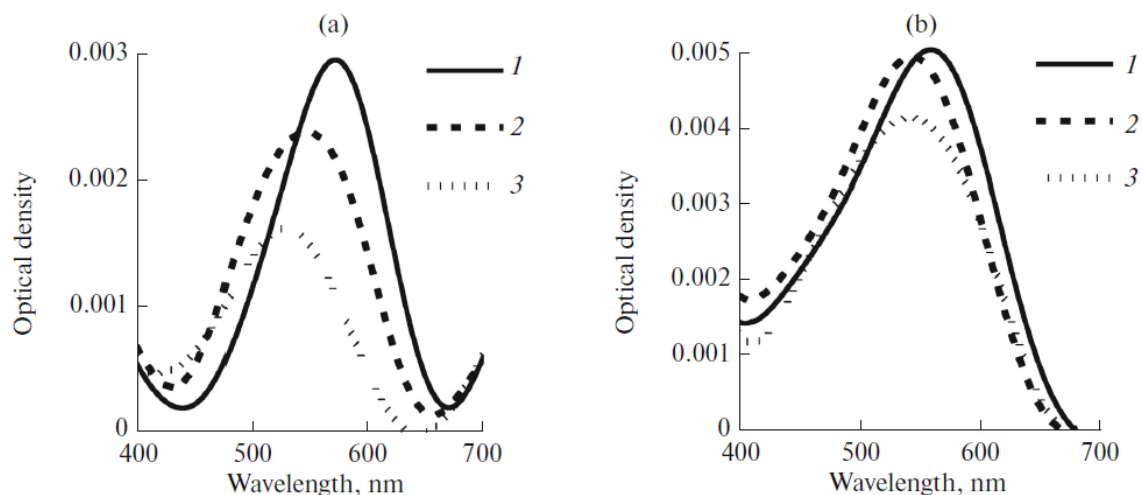


**Fig. 11.** Electronic-absorption spectra of multilayer LB films on the surface of quartz. (a) C12 (18 layers) and (b) C18 (10 layers). (1) LB films of ligands; LB films of ligands conditioned in 0.1 mM in aqueous  $\text{Hg}(\text{ClO}_4)_2$  solution for (2) 10 and (3) 20 s. Transfer pressure: 20 mN/m.

#### 4. CONCLUSIONS

This work presents an original approach to obtaining highly sensitive ultrathin film sensors relies on molecular design of surface-active modular molecules from a signal anthraquinone block, hydrophobic radicals, and polar receptor groups, the number and size of which being configured in accordance with the sensor type. This approach was employed to develop a series of chromophoric receptor molecules of different lipophilicity (HLB) that are used to obtain sensitive and selective planar elements for optical sensors.

Complexing properties of amphiphilic ligands of a new family in the Langmuir monolayer have been studied in detail. The mechanism of interaction between cations and the sublayer of receptor groups has been suggested on the basis of compression isotherms and the data of fiber-optic spectroscopy. Selectivity of ligands with respect to mercury and copper cations has been shown.

Sensor characteristics of multilayer Langmuir–Blodgett films on the quartz surface have been studied; it is shown that their sensitivity with respect to metal cations is two orders of magnitude higher than for the liquid counterparts. An increase in lipophilicity of the ligands allowed enhancing the stability of operation of sensors in aqueous media.

Thus, new amphiphilic anthraquinone derivatives have been used to developed high-performance selective liquid and solid-state film sensors for determination of mercury and copper cations in aqueous solutions.

## **ACKNOWLEDGMENTS**

This work was supported by the Russian Foundation for Basic Research (projects n° 16-29-05272 and 17-53-16018) and Program I.8 P of the Presidium of the Russian Academy of Sciences.

## REFERENCES

1. Li, S., Singh, J., Li, H., and Banerjee, I.A., *Biosensor Nanomaterials*, Hoboken, NJ: John Wiley and Sons, 2011.
2. Gumpu, M.B., Sethuraman, S., Krishnan, U.M., and Rayappan, J.B.B., *Sens. Actuators, B*, 2015, vol. 213, pp. 515–533.
3. Li, M., Gou, H., Al-Ogaidi, I., and Wu, N., *ACS Sustainable Chem. Eng.*, 2013, vol. 1, no. 7, pp. 713–723.
4. Mahbub, K.R., Krishnan, K., Naidu, R., Andrews, S., and Megharaj, M., *Ecol. Indic.*, 2017, vol. 74, pp. 451–462.
5. Schaefer, J.K., Szczuka, A., and Morel, F.M.M., *Environ. Sci. Technol.*, 2014, vol. 48, no. 5, pp. 3007–3013.
6. Gribble, M.O., Karimi, R., Feingold, B.J., Nyland, J.F., O’Hara, T.M., Gladyshev, M.I., and Chen, C.Y., *J. Mar. Biol. Assoc. U. K.*, 2016, vol. 96, pp. 43–59.
7. Zadnurd, R., Akbari-Moghaddam, P., and Darvishi, S., *Supramol. Chem.*, 2017, vol. 29, no. 1, pp. 17–23.
8. Yu, J.G., Yue, B.Y., Wu, X.W., Liu, Q., Jiao, F.P., Jiang, X.Y., and Chen, X.Q., *Environ. Sci. Pollut. Res.*, 2016, vol. 23, no. 6, pp. 5056–5076.
9. Hordyjewska, A., Popiolek, Ł., and Kocot, J., *Biometals*, 2014, vol. 27, no. 4, pp. 611–621.
10. Scheiber, I.F., Mercer, J.F., and Dringen, R., *Prog. Neurobiol.*, 2014, vol. 116, pp. 33–57.
11. Ahuja, A., Dev, K., Tanwar, R.S., Selwal, K.K., and Tyagi, P.K., *J. Trace Elem. Med. Biol.*, 2015, vol. 29, pp. 11–23.
12. Wu, J., Ricker, M., and Muench, J., *J. Am. Board Fam. Med.*, 2006, vol. 19, no. 2, pp. 191–194.
13. Griffin, W.C., *J. Soc. Cosmet. Chem.*, 1946, vol. 1, pp. 311–326.
14. Ranyuk, E., Uglov, A., Meyer, M., Bessmertnykh-Lemeune, A., Denat, F., Averin, A., Beletskaya, I., and Guillard, R., *Dalton Trans.*, 2011, vol. 40, no. 40, pp. 10491–10502.
15. Arslanov, V., Ermakova, E., Michalak, J., Bessmertnykh-Lemeune, A., Meyer, M., Raitman, O., Vysotskij, V., Guillard, R., and Tsivadze, A., *Colloids Surf., A*, 2015, vol. 483, pp. 193–203.
16. Fukuda, K., Nakahara, H., and Kato, T., *J. Colloid Interface Sci.*, 1976, vol. 54, no. 3, pp. 430–438.
17. O’Hanlo, D. and Forster, R.J., *Langmuir*, 2000, vol. 16, pp. 702–707.
18. Nakahara, H., *Stud. Interface Sci.*, 1996, vol. 4, pp. 71–108.

19. Selector, S., Fedorova, O., Lukovskaya, E., Anisimov, A., Fedorov, Y., Tarasova, N., Raitman, O., Fages, F., and Arslanov, V., *J. Phys. Chem. B*, 2012, vol. 116, no. 5, pp. 1482–1490.
20. Ranyuk, E., Ermakova, E.V., Bovigny, L., Meyer, M., Bessmertnykh-Lemeune, A., Guillard, R., Rousselin, Y., Tsivadze, A.Y., and Arslanov, V.V., *New J. Chem.*, 2014, vol. 38, no. 1, pp. 317–329.
21. Selektor, S., Shokurov, A., Raitman, O., Sheinina, L., Arslanov, V., Birin, K., Gorbunova, Y.G., and Tsivadze, A.Y., *Colloid J.*, 2012, vol. 74, no. 3, pp. 334–345.
22. Ermakova, E., Enakieva, Yu., Zvyagina, A., Gorbunova, Yu., Kalinina, M., and Arslanov, V., *Macroheterocycles*, 2016, vol. 9, pp. 378–386.
23. Ermakova, E., Meshkov, I., Enakieva, Yu., Zvyagina, A., Ezhov, A., Mikhaylov, A., Gorbunova, Yu., Kalinina, M., and Arslanov, V., *Surf. Sci.*, 2017, vol. 660, pp. 39–46.
24. Zotova, T., Arslanov, V., and Gagina, I., *Thin Solid Films*, 1998, vol. 326, pp. 223–226.
25. Kalinina, M.A., Arslanov, V.V., Tsar'kova, L.A., and Rakhnyanskaya, A.A., *Colloid J.*, 2000, vol. 62, no. 5, pp. 545–549.
26. Kalinina, M.A., Arslanov, V.V., Zheludeva, S.I., and Tereschenko, E.Y., *Thin Solid Films*, 2005, vol. 472, no. 1, pp. 232–237.
27. Wang, F., Wei, X., Wang, C., Zhang, S., and Ye, B., *Talanta*, 2010, vol. 80, no. 3, pp. 1198–1204.
28. Ludwig, R., *Fresenius' J. Anal. Chem.*, 2000, vol. 367, no. 2, pp. 103–128.
29. Riegler, H. and Spratte, K., *Thin Solid Films*, 1992, vol. 210, pp. 9–12.
30. Raudino, A. and Pignataro, B., *J. Phys. Chem. B*, 2007, vol. 111, no. 31, pp. 9189–9192.
31. Elenskiy, A.A., Turygin, D.S., Arslanov, V.V., and Kalinina, M.A., *Nanotechnol. Russ.*, 2009, vol. 4, pp. 275–280.
32. Arslanov, V.V., Sheinina, L.S., and Kalinina, M.A., *Prot. Met.*, 2008, vol. 44, no. 1, pp. 1–21.
33. Watson, S.M.D., Coleman, K.S., and Chakraborty, A.K., *ACS Nano*, 2008, vol. 2, no. 4, pp. 643–650.
34. Kalinina, M.A., Raitman, O.A., Turygin, D.S., Selektor, S.L., Golubev, N.V., and Arslanov, V.V., *Russ. J. Phys. Chem. A*, 2008, vol. 82, no. 8, pp. 1334–1342.
35. Zhavnerko, G. and Marletta, G., *Mater. Sci. Eng., B*, 2010, vol. 169, pp. 43–48.
36. Xu, G., Bao, Z., and Groves, J.T., *Langmuir*, 2000, vol. 16, no. 4, pp. 1834–1841.
37. Cao, Y., Wei, Z., Liu, S., Gan, L., Guo, X., Xu, W., Steigerwald, M.L., and Liu, Z., *Angew. Chem.*, 2010, vol. 122, no. 36, pp. 6463–6467.

38. Kim, J., *Pure Appl. Chem.*, 2002, vol. 74, no. 11, pp. 2031–2044.
39. Prabhakaran, D., Yuehong, Ma., Nanjo, H., and Matsunaga, H., *Anal. Chem.*, 2007, vol. 79, pp. 4056–4065.
40. Prabhakaran, D., Nanjo, H., and Matsunaga, H., *Anal. Chim. Acta*, 2007, vol. 601, pp. 108–117.